TÜBİTAK

Turkish Journal of Physics

http://journals.tubitak.gov.tr/physics/

Research Article

Turk J Phys
(2020) 44: 384 – 393
© TÜBİTAK
doi:10.3906/fiz-2003-17

Investigating above-bandgap and below-bandgap optical transition in GaBiAs epilayers by photoreflectance spectroscopy

Ömer DÖNMEZ*, **Ayşe EROL**
Department of Physics, Faculty of Science, Istanbul University, Istanbul, Turkey

Received: 25.03.2020 • **Accepted/Published Online:** 25.06.2020 • **Final Version:** 31.08.2020

Abstract: We present optical identification of deep level defects in as-grown and annealed $GaBixAs_{1-x}$ (x = 0, 0.013 and 0.015) alloys grown at different temperatures (220 °C and 320 °C) by using photo-modulated reflectance (PR) spectroscopy and photoluminescence (PL). The PR measurements are employed at above- and below-bandgap excitations, and the PR line-shape is analyzed by the third derivative functional form (TDFF). The PR at below-bandgap excitation reveals transitions at 0.757 ±0.001 eV and 0.710 ±0.002 eV at 30K and 300K, respectively. Franz-Keldysh oscillations are observed in all samples under above-bandgap excitation at PR measurements, and the built-in electric field, which may originate from the charged As-antisite defects is calculated from local extrema points in the PR spectra. The decrease in the built-in electric field after thermal annealing is explained with decreased point defect density.

Key words: Dilute bismide alloys, GaBiAs, deep level defect, antisite defect, photoreflectance

1. Introduction

GaBiAs alloys are recent members of the highly mismatched alloys (HMAs) family and attract a great deal of interest due to their unique properties and potential in terahertz and spintronic applications [1–5]. The bismuth-related modifications of the band structure and bandgap energy of GaBiAs provide flexibility for bandgap engineering and make GaBiAs attractive as promising candidates for optoelectronic applications [3]. As it has been experienced in all members of the HMAs [6,7], GaBiAs alloys suffer from low temperature (LT) growth-related crystal defects and disorders such as ~0.4 eV, ~0.55 eV, ~0.65-0.7 eV and ~0.8 eV [8–10], among which some have also been reported for LT-GaAs. These defects may be detrimental to the optical and electrical properties of GaBiAs alloys; therefore, they should be identified before fabrication of GaBiAs-based optoelectronic/electronic devices. When the cross-section of the defects is sufficiently high, the levels of the existing defects may be probed by optical techniques such as photoluminescence (PL). The emission-like spectrum of PL measurements is a powerful technique at low temperatures for determining bandgap energy and identifying trap levels. However, nonradiative transitions quench PL intensity. Therefore, it is difficult to observe room temperature PL if the material quality is not good enough. It is well-known that GaBiAs suffer from defects located at around band edges and deep-level traps, resulting in nonradiative transitions and decreased radiative recombination rates [9,11–14]. As for measuring defect-assisted PL from a sample, the cross-section of the defect should be high [15]. If the cross-section of the defect is low, defect-assisted PL cannot be detected even at very low temperatures.

*Correspondence: omerdonmez@istanbul.edu.tr

PR spectroscopy has proven to be a powerful and nondestructive experimental technique for studying and characterizing bulk and low-dimensional semiconductors. PR spectroscopy is sensitive to surface and interface fields, e.g., built-in electric fields, and optical transitions with its sharp derivative-like spectrum. The derivative-like characteristic of the PR spectrum enables determining a variety of transitions, which corresponds to bandgap, alloy inhomogeneity and defect-related transitions even at room temperature. Surface or interface electric field sensitivity of PR spectroscopy also allows us to probe the existence of charged states in semiconductor interfaces. If the internal electric field is large enough, oscillatory behavior and Franz-Keldysh oscillations (FKOs) at the PR spectrum show themselves above the bandgap energy. It is well-known that FKOs are evidence of large built-in electric fields [16], and analyzing this spectral property of PR provides information about the amplitude of the built-in electric field [17]. For a doped bulk GaAs, surface electric field gives rise to FKOs with an amplitude of a few tenths kV/cm [18,19].

On the other hand, for an undoped sample, determination of the built-in electric field with an amplitude of a few tenth kV/cm may be an indication of another source, which leads to a built-in electric field in an undoped sample. Recent studies have shown that undoped GaBiAs alloys have charged defects with different activation energies [8,9], which may be the source of a built-in electric field. Therefore, we use the PR technique to identify whether charged traps exit in GaBiAs alloys. Observation of FKOs in PR line-shape indicates that the nature of the defect is not neutral but charged. Even though PR provides information about the levels of existing defects, the origin of the defects cannot be solely determined by using this technique.

In this article, we present optical identification of defects in undoped as-grown and annealed GaBiAs alloys grown by MBE. The PR results at below-bandgap excitation reveal that defect-assisted optical transitions are the source of the observed spectrum, and the energy levels of these defect are determined approximately as 0.757 eV and 0.710 eV for 30K and 300K, respectively. The observed FKOs in PR spectrum reveal that the defect is charged, not neutral. To find out that if the defect is Bi-related, PR measurements on LT growth of GaAs and GaBiAs are compared at below-bandgap and above-bandgap excitation at 30 K and 300 K.

2. Materials and methods

$GaBi_xAs_{1-x}$ samples that were used in this study were grown by MBE with various Bi concentrations (x =0, 0.013, 0.015). To investigate the effects of bismuth incorporation on optical properties, we also grew a Bi-free sample at 220 °C as a reference. All samples were grown on a semiinsulating GaAs substrate. After the growth of a GaAs buffer layer at 580 °C, the temperature was reduced to 220 °C, and 320 °C for the growth of the GaBiAs samples, while the Bi-free sample was grown at 220 °C on the GaAs layer. The As/Ga flux ratio was close to the stoichiometric value for GaBiAs layers, as required for efficient Bi incorporation and ~3 for the Bi-free sample. The bismuth concentrations were determined by XRD. All samples that were investigated in this study are listed in Table 1. Rapid thermal annealing was carried out at 600 °C for 60 s.

Table 1. Properties of the samples used in the study.

Sample	Growth temperature (°C)	Bi%	Code	Thickness (nm)
GaAs	220	0	R220	230
GaBiAs	220	1.5	B220	270
	320	1.3	B320	

PR in bright configuration mode was carried out by using a 940 nm diode laser at 100 mW (below-bandgap excitation) and a 514 nm Ar-ion laser at 60 mW (above-bandgap excitation) as pump sources, and a 100 W halogen lamp was used as a probe source. The pump source was modulated at a frequency of 167 Hz. A 0.5 m monochromator dispersed the reflected light. To avoid second order contributions, a long pass filter with a 715 nm cut-on for GaAs sample (Newport FSQ-RG715) and a 1000 nm cut-on (Newport FSQ-RG1000) during PR measurements of GaBiAs samples were placed in front of the entrance slit of the monochromator.

The PR signals were detected by a TE-cooled Amplified InGaAs and a Si photodiode by using a conventional lock-in amplifier detection technique. To increase the signal/noise ratio, the PR signal was taken 4 times for each wavelength, and then, the averaged value was recorded, and the wavelength sweep rate was chosen as 0.25 nm/min during the experiments. Slit width of monochromator is set as 0.3 mm for above band gap transition and as 0.75 mm for below band gap transition.

The line-shape of the PR spectra was fitted by using TDFF [20–23],

$$\frac{\Delta R}{R} = Ae^{-i\emptyset}\left(E - E_G + i\Gamma\right)^{-m}$$

where E is the photon energy; $A, \emptyset$, E_G and Ã are the amplitude, phase, optical transition energy, and line-broadening, respectively. m represents the type of the critical point depending on the dimensionality of the structure, and its value was taken as 2.5 for the best fit.

PL measurement was made by using a 514 nm line of an Ar-ion laser, and an LN_2 cooled InGaAs photomultiplier tube was used to detect PL signals. A lock-in amplifier recorded PL signals.

3. Results and discussion

Figure 1 shows the XRD spectra of the GaBiAs samples (B220 and B320). The sharp center peaks corresponded to diffraction from the GaAs buffer and SI GaAs substrate layers, while the peaks located at –460 and –385 arcsec originated from the GaBiAs-containing layer for the samples B220 and B320, respectively. There were fringes in both spectra, which indicated that both the GaBiAs layers have homogeneous Bi concentration. The Bi concentration of the B220 and B320 samples was determined as 1.5% and 1.3%, respectively as seen in Figure 1.

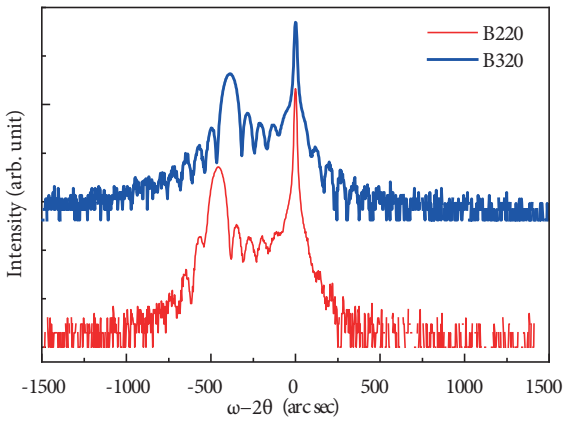

Figure 1. XRD spectra of the B220 (black line) and B320 (red line) samples.

Figure 2a shows the PL spectra of the as-grown and thermally annealed samples at 30 K. The PL signal quenched above 100 K for the as-grown sample and above 200 K for the annealed sample B320. We could not observe any PL signal for the sample B220 even at 30 K. It was reported that a small amount of Bi as a surfactant enhances the structural and optical quality of GaBiAs alloys [14,24,25]. As the growth temperature decreases, even Bi atoms behave as a surfactant, so, a higher nonradiative defect density in GaBiAs, which is grown at very low temperatures, may be expected. Increased nonradiative defect density drastically reduces the radiative recombination rates and causes no observation of PL emissions even at 30 K [26,27]. The reason for not observing PL from the sample B220 even at low temperatures may be related to the lower growth temperature. This was less effective for the sample grown at a higher temperature (B320). Therefore, the as-grown B320 sample emitted up to 110 K due to both surfactant roles of Bi atoms and higher growth temperature. As for the annealed sample B320, the PL signal quenched above 200 K, and the PL intensity was higher than that of the as-grown sample (see Figure 2). A negligibly small redshift (8 meV) of the PL peak energy was observed as an effect of thermal annealing for the sample R320. Optical transition energies and FWHM values of PL peaks were determined to be as 1.164 eV and 1.156 eV and 190 meV and 120 meV for the as-grown and thermally annealed B320 samples, respectively. The FWHM values were larger than the recent values observed for GaBiAs, which emitted at room temperature [11,27]. As seen in Figure 1, B320 was a homogenous material; therefore, a broader line-width might have been originated from the localized states in the bandgap.

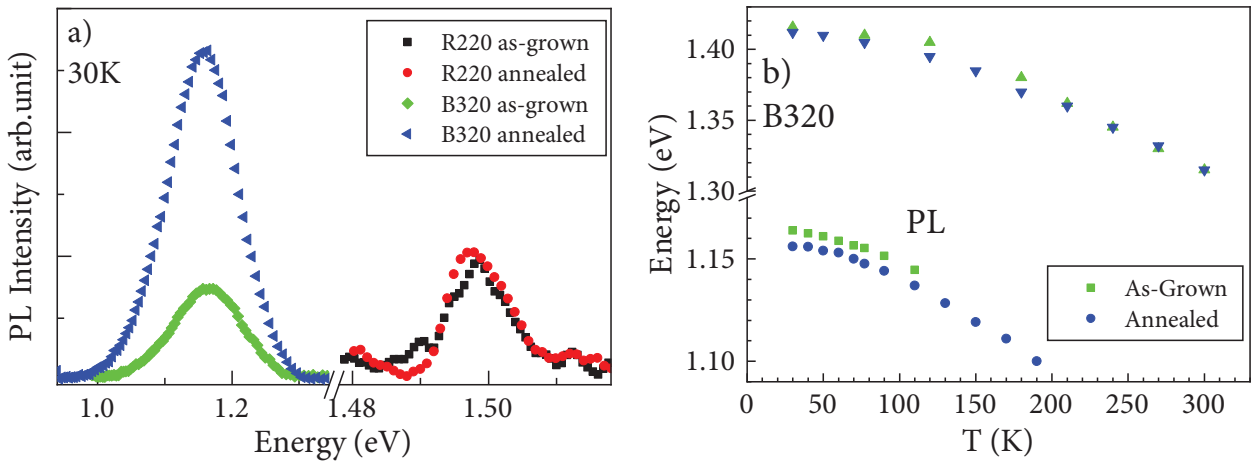

Figure 2. a) PL spectra of as-grown and thermally annealed R220 and B320 at 30 K. The PL spectra of R220 samples are multiplied by 20 for clarity. b) Temperature dependence of PL peak and PR transition energy of as-grown and annealed sample B320.

The optical transition energy of the as-grown and annealed reference sample, R220, was about 1.500 eV, and it could not be measured at temperatures higher than 30 K by using PL. In contrast to the PL results, the temperature dependence of the optical transition energy of all the samples could be obtained with TDFF-fitted PR as given for the as-grown B320 in Figure 2b. This result also confirmed the sensitivity of PR spectroscopy for our samples. We will not further discuss the temperature dependence of the optical transitions that were observed in PL and PR measurements because it is out of the scope of this paper and widely discussed in the literature [11,12].

It is well-known that the composition dependence of the bandgap of GaBiAs is 60–90 meV/Bi% [20,27,28]. The PL peak energy ($\sim$1.500 eV at 30 K) of the R220 corresponded to the bandgap of the GaBiAs with 1.5%

Bi, which was consistent with the composition obtained from XRD. The PL peak energy for B320 with 1.3% Bi was at 1.164 eV, which was higher than the expected shrinkage value of the bandgap of GaBiAs. Therefore, this transition could be assigned to the bandgap of not B320 but defect-assisted radiative recombination. The observed higher transition energy at the PR spectrum (1.412 eV) given in Figure 2b matched with the expected bandgap value of B320. The energy difference between PL peak energy and band gap energy determined from the PR was about 0.25 eV, which was also observed in the DLTS measurement [8], but its origin has not been identified yet.

To further investigate the presence of defects, we carried out PR measurements with a 940 nm diode laser as a pump source to excite the samples with an energy level that was lower than the expected bandgap energy of the samples. Figure 3 shows the experimental and TDFF-fitted PR spectra of the as-grown samples at 30 K and 300 K. The TDFF-fitted PR energies were almost the same for all samples and calculated as 0.757 $\pm$0.001 eV and 0.710 $\pm$0.002 eV for 30 K and 300 K, respectively, and the transition energies redshifted with an amount of ~47 meV between 30 K and 300 K. The PR linewidths of this signal were ~0.8 meV and ~2.5 meV for 30 K and 300 K, respectively. The different kinds of PR line-shapes that were observed were induced by the phase shift ($\emptyset$). It is worth noting that a diode laser did not have enough energy to excite the GaAs layer of the samples, and a long pass filter with a cut-on wavelength of 1000 nm (1.24 eV) was used in the PR measurements for the GaBiAs samples. Therefore, the observed transitions could not be related to the second order of the GaAs bandgap energy.

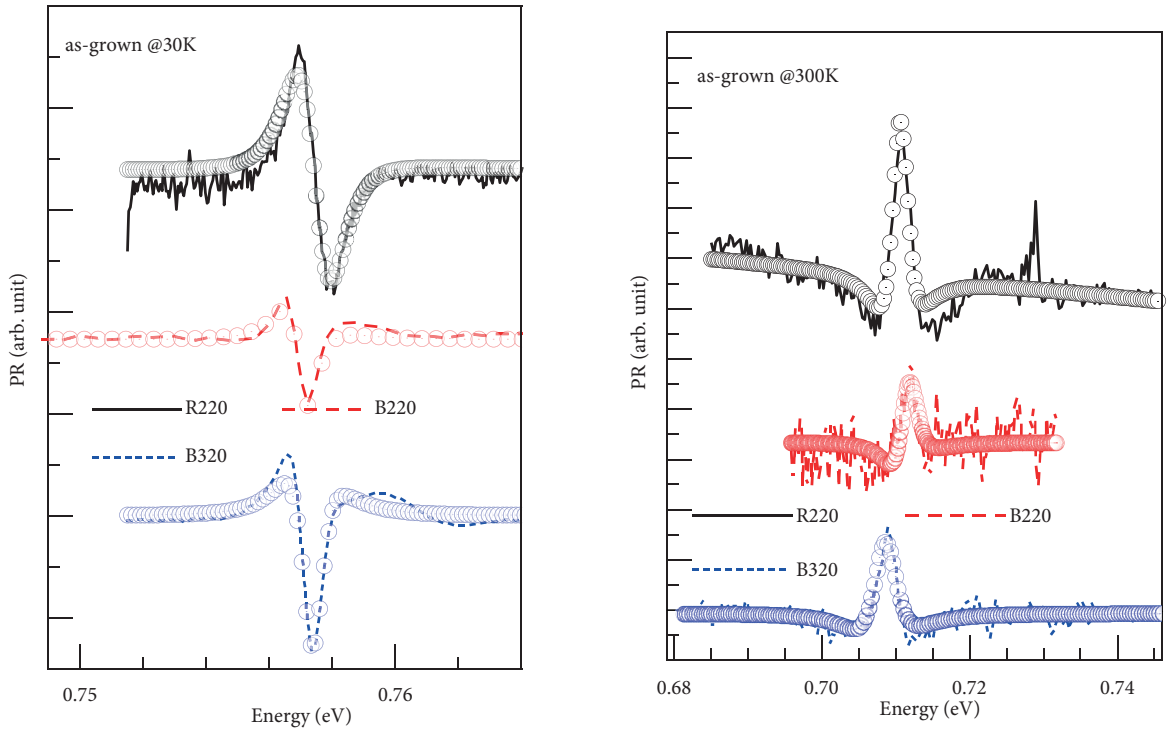

Figure 3. Experimental and TDFF-fitted spectra of as-grown R220, B220 and B320 samples at a) 30 K and b) 300 K. Differently colored types of lines and red circles represent the experimental and TDFF-fitted PR spectra, respectively.

It is well known that LT GaAs has a charged As_{Ga} point defect located in the bandgap at around 0.5–0.72 eV depending on defect concentration [29–31]. There are a few studies on identification of Bi-related

defects in GaBiAs. Kunzer et al. showed that liquid encapsulation in Czochralski growth GaAs doped with Bi has well-known As_{Ga}, $Bi_{Ga}^{0/+}$ and $Bi_{Ga}^{+/++}$ defects, and their activation energies are 0.7 eV, 0.35–0.5 eV, and 0.65–0.7 eV from conduction band edge, respectively, but Bi_{Ga} defect density is lower than that of As_{Ga}. They determined that the maximum allowed Bi_{Ga} defect concentration has to be 10% of the total Bi amount [32]. However, Ciatto et al. determined that the upper limit of the Bi_{Ga} defect concentration is 5% of the total Bi concentration in GaBiAs grown by MBE [33]. Mooney et al. showed that GaBiAs alloys grown by MBE consist of $Bi_{Ga}^{0/+}$ defects, and their activation energy is 0.35–0.5 eV [9,10]. Recently, Gelczuk et al. reported a similar kind of defects in GaBiAs alloys without identifying the type of the charged defects [34]. Also, Alberi et al. report the effect of the deep and shallow defect state on the optical transition, but they did not discuss charged state of these defects [35]. According to these limited recent studies on deep levels and the other recent studies in the literature [36–38], activation energies of the well-known As_{Ga} and $Bi_{Ga}^{+/++}$ defects are close to each other, and to identify the defect type, it is necessary to use different techniques such as positron lifetime spectroscopy [39]. Referring to these studies and considering the experimental findings from PR, the TDFF-fitted transition energies at about 0.7 eV may be attributed to the As_{Ga} and not the $Bi_{Ga}^{+/++}$ defect-related transition, since the reference sample (Bi-free, GaAs) also had the same optical transition property. It is worth noting that PR transition at ~0.7 eV could not be observed in the GaAs grown at the ideal growth temperature (570–570 °C) [40].

Observation of FKOs in undoped materials indicates the presence of charged antisite defects; therefore, we also carried out PR measurements at higher energies (above-bandgap excitation) than the bandgap energy of GaAs and GaBiAs to investigate the occurrence of FKOs. Figure 4 shows the high-energy part of the experimental spectra of the as-grown R220, B220 and B320 samples. In Figure 4, FKOs appear at a higher energy than the bandgap of the samples. The built-in electric field values related to $As_{Ga}^{+/++}$ defect were determined from the slope of the $4/3\pi\ (E_n - E_G)^{3/2} - peak\ number$ curves, which were obtained from the local extrema points of FKOs [16] and are given in Table 2. The calculated built-in electric field values were 16 kV/cm, 12 kV/cm and 13 kV/cm for as-grown R220, B220, and B320, respectively.

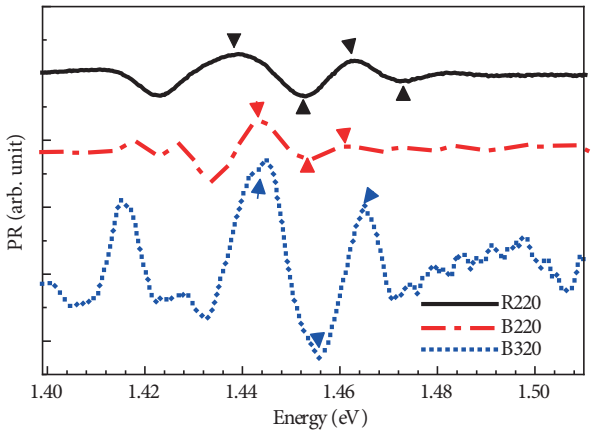

Figure 4. Experimental PR spectra $GaBi_xAs_{1-x}$ at room temperature. The arrows show the peak value used in built-in electric fields calculation. Colored arrows show energy extrema points of the FKOs.

Table 2. Built-in electric field values for as-grown and annealed samples.

Sample	Electric field (kV/cm) @300 K	
	as-grown	annealed
R220	16 ±0.2	15 ±0.2
B220	12 ±0.6	12 ±0.5
B320	13 ±1.3	10 ±1.2

The highest built-in electric field was obtained for the reference sample (R220). Incorporation of the Bi atom into GaAs not only changes the bandgap of the alloy but also behaves as a surfactant during growth, which increases crystal quality and reduces point defect density in the alloys. Therefore, observation of lower built-in electric fields for the samples B220 and B320 was an indication of enhanced crystal quality [41,42]. The built-in electric fields in the samples B220 and B320 were close to each other within the confines of experimental error.

To understand the effects of thermal treatment on charged defect states, rapid thermal annealing was performed. Figure 5 shows the experimental and TDFF-fitted PR spectra of thermally annealed R220, B220 and B320 samples at 30 K and 300 K. The transition energies and the linewidths of the TDFF of the PR spectra for the annealed samples were almost the same in comparison to the results of the as-grown samples. The optical transition energy shift was also the same as the value of 47 meV between 30 K and 300 K. The built-in electric field tended to decrease after thermal annealing as shown in Table 2.

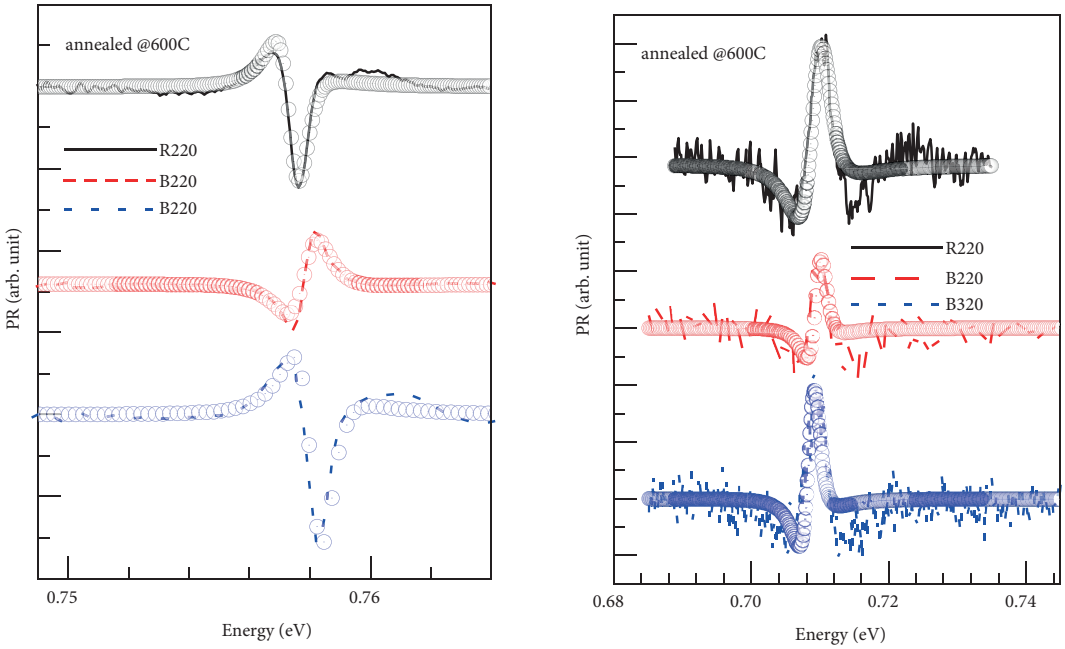

Figure 5. PR spectra and TDFF-fitted results of annealed $GaBi_xAs_{1-x}$ at a) 30 K and b) 300 K. Differently colored different types of lines and red circles represent experimental and TDFF-fitted PR spectra, respectively.

It was reported that thermal annealing causes precipitation of the As_{Ga} defect. Therefore, it reduces As_{Ga} defect density [30,43,44]. The reason for the decreased built-in electric field may be related to the decreased density of the charged point defects for the B320 sample.

4. Conclusion

In this study, we determined defect-assisted optical trans itions in as-grown and annealed $GaBi_xAs_{1-x}$ (x = 0, 0.013, 0.015) alloys by using the PR and PL methods. The samples were grown at different temperatures (220 °C and 320 °C) by MBE. The PR measurements performed at below-bandgap excitation enabled us to observe the conduction band in defect-related transitions. Steady-state charged As_{Ga} defect energies were obtained from the TDFF PR line-shape as 0.757 ±0.001 eV and 0.710 ±0.002 eV for 30 K and 300 K, respectively. The built-in electric field was determined from FKOs and tended to decrease with the incorporation of Bi and the thermal annealing process.

Acknowledgement

This study was supported by the Scientific Research Projects Coordination Unit of İstanbul University (Project no: ONAP-52321). We would like to thank J. Puustinen, J. Hilska, and Mircea Guina for growing the samples and valuable contribution to this study.

References

1 Arlauskas A, Svidovsky P, Bertulis K, Adomavičius R, Krotkus A. GaAsBi photoconductive terahertz detector densitivity at long excitation wavelengths. Applied Physics Express 2012; 5 (2): 022601. doi: 10.1143/APEX.5.022601

2 Bertulis K, Krotkus A, Aleksejenko G, Pačebutas V, Adomavičius R et al. GaBiAs: A material for optoelectronic terahertz devices. Applied Physics Letters 2006; 88 (20): 201112. doi: 10.1063/1.2205180

3 Sweeney SJ, Jin SR. Bismide-nitride alloys:Promising for efficient light emitting devices in the near- and mid-infrared. Journal of Applied Physics 2013; 113 (4): 043110. doi: 10.1063/1.4789624

4 Marko IP, Ludewig P, Bushell ZL, Jin SR, Hild K et al. Physical properties and optimization of GaBiAs/(Al)GaAs based near-infrared laser diodes grown by MOVPE with up to 4.4% Bi. Journal of Physics D: Applied Physics 2014; 47 (34) : 345103. doi:10.1088/0022-3727/47/34/345103

5 Prando GA, Orsi GV, Puustinen J, Hilska J, Alghamdi HM et al. Exciton localization and structural disorder of $GaAs_{1-x}Bi_x$/GaAs quantum wells grown by molecular beam epitaxy on (311)B GaAs substrates. Semiconductor Science and Technology 2018; 33 (8): 084002. doi:10.1088/1361-6641/aad02e

6 Buyanova IA, Chen WM, Monemar B, Xin HP, Tu CW. Effect of growth temperature on photoluminescence of GaNAs/GaAs quantum well structures. Applied Physics Letters 1999; 75 (24): 3781. doi:10.1063/1.125454

7 Carrère H, Marie X, Barrau J, Amand T, Sen-Bouzid S et al. Band structure calculations for dilute nitride quantum wells under compressive or tensile strain. Journal of Physics: Condensed Matter 2004; 16 (31): S3215-S3227. doi:10.1088/0953-8984/16/31/016

8 Jiang Z, Beaton DA, Lewis RB, Basile AF, Tiedje T et al. Deep level defects in $GaAs_{1-x}Bi_x$/GaAs heterostructures. Semiconductor Science and Technology 2011; 26 (5): 055020. doi:10.1088/0268-1242/26/5/055020

9 Mooney PM, Watkins KP, Jiang Z, Basile AF, Lewis RB et al. Deep level defects in n-type GaAsBi and GaAs grown at low temperatures. Journal of Applied Physics 2013; 113 (13):133708. doi:10.1063/1.4798237

10 Mooney PM, Tarun M, Beaton DA, Mascarenhas A, Alberi K. Deep level defects in dilute GaAsBi alloys grown under intense UV illumination. Semiconductor Science and Technology 2016; 31 (8): 085014. doi:10.1088/0268-1242/31/8/085014

11 Mohmad AR, Bastiman F, Hunter CJ, Richard RD, Sweeney SJ et al. Localization effects and band gap of GaAsBi alloys. Physica Status Solidi (B) 2014; 251(6):1276-1281. doi:10.1002/pssb.201350311

12 Imhof S, Thränhardt A, Chernikov A, Koch M, Köster NS et al. Clustering effects in Ga(AsBi). Applied Physics Letters 2010; 96 (13): 131115. doi:10.1063/1.3374884

13 Imhof S, Wagner C, Chernikov A, Koch M, Kolata K et al. Evidence of two disorder scales in Ga(AsBi). Physica Status Solidi (B) 2011; 248 (4):851. doi:10.1002/pssb.201000835

14 Fuyuki T, Kashiyama S, Tominaga Y, Oe K, Yoshimoto M. Deep-hole traps in p-type $GaAs_{1-x}Bi_x$ grown by molecular beam epitaxy. Japanese Journal of Applied Physics 2011; 50 (8): 080203. doi:10.1143/JJAP.50.080203

15 Yu PW, Robinson GD, Sizelove JR, Stutz CE. 0.8-eV photoluminescence of GaAs grown by molecular-beam epitaxy at low temperatures. Physical Review B 1994; 49 (7): 4689. doi:10.1103/PhysRevB.49.4689

16 Shen H, Pollak FH. Generalized Franz-Keldysh theory of electromodulation. Physical Review B 1990; 42 (11): 7097. doi:10.1103/PhysRevB.42.7097

17 Misiewicz J, Sęk G, Kudrawiec R, Sitarek P. Semiconductor heterostructure and device structures investigated by photoreflectance spectroscopy. Materials Science 2003; 21(3):263-320

18 Kudrawiec R, Sek G, Sitarek P, Ryczko K, Misiewicz J et al. Three beam photoreflectance as a powerful method to investigate semiconductor heterostructures. Thin Solid Films 2004; 450(1): 71-74. doi:10.1016/j.tsf.2003.10.054

19 Shen H, Dutta M, Fotiadis L, Newman PG, Moerkirk RP et al. Photoreflectance study of surface Fermi level in GaAs and GaAlAs. Applied Physics Letters 1990; 57(20):2118. doi:10.1063/1.103916

20 Donmez O, Kara K, Erol A, Akalın E, Makhloufi H et al. Thermal annealing effects on optical and structural properties of GaBiAs epilayers: Origin of the thermal annealing-induced redshift in GaBiAs. Journal of Alloys and Compounds 2016; 686: 976-981. doi:10.1016/j.jallcom.2016.05.326

21 Aspnes DE. Third-derivative modulation spectroscopy with low-field electroreflectance. Surface Science 1973; 37:418-442. doi:10.1016/0039-6028(73)90337-3

22 Pollak FH, Shen H. Modulation spectroscopy of semiconductors:Bulk/thin film, microstructures, surfaces/interfaces and devices. Materials Science and Engineering: R: Report 1993; 10 (7-8): 275-374. doi:10.1016/0927-796X(93)90004-M

23 Misiewicz J, Sek G, Kudrawiec R, Sitarek P. Photomodulated reflectance and transmittance: Optical characterisation of novel semiconductor materials and device structures. Thin Solid Films 2004; 450(1):14-22. doi:10.1016/j.tsf.2003.10.041

24 Puustinen J, Wu M, Luna E, Laukkanen P, Schramm A et al. Variation of lattice constant and cluster formation in GaAsBi. Journal of Applied Physics 2013; 114(24): 243504. doi: 10.1063/1.4851036

25 Yoshimoto M, Murata S, Chayahara A, Horino Y, Saraie J et al. Metastable GaAsBi alloy grown by molecular beam epitaxy. Japanese Journal of Applied Physics 2003; 42 (10B): L1235-L1237. doi:10.1143/JJAP.42.L1235

26 Beaton DA, Mascarenhas A, Alberi K. Insight into the epitaxial growth of high optical quality $GaAs_{1-x}Bi_x$. Journal of Applied Physics 2015; 118(23): 235701. doi: 10.1063/1.4937574

27 Sarcan F, Dönmez Ö, Kara K, Erol A, Akalın E et al. Bismuth-induced effects on optical, lattice vibrational, and structural properties of bulk GaAsBi alloys. Nanoscale Research Letters 2014; 9(1): 119. doi:10.1186/1556-276X-9-119

28 Bahrami-Yekta V, Tiedje T, Masnadi-Shirazi M. MBE growth optimization for $GaAs_{1-x}Bi_x$ and dependence of photoluminescence on growth temperature. Semiconductor Science and Technology 2015; 30 (9):094007. doi:10.1088/0268-1242/30/9/094007

29 Bourgoin JC, Neffati T. The energy level of the EL2 defect in GaAs. Solid-State Electronics 1999; 43(1): 153-158. doi:10.1016/S0038-1101(98)00199-3

30 Look DC. Molecular beam epitaxial GaAs grown at low temperatures. Thin Solid Films 1993; 231 (1-2): 61-73. doi:10.1016/0040-6090(93)90703-R

31 Look DC, Fang ZQ, Sizelove JR, Stutz CE. New As_{Ga} related center in GaAs. Physical Review Letters 1993; 70 (4):465. doi:10.1103/PhysRevLett.70.465

32 Kunzer M, Jost W, Kaufmann U, Hobgood HM, Thomas RN. Identification of the Bi_{Ga} heteroantisite defect in GaAs:Bi. Physical Review B 1993; 48(7): 4437. doi: 10.1103/PhysRevB.48.4437

33 Ciatto G, Alippi P, Amore Bonapasta A, Tiedje T. How much room for Bi_{Ga} heteroantisites in $GaAs_{1-x}Bi_x$? Applied Physics Letters 2011; 99(14): 141912. doi:10.1063/1.3647635

34 Gelczuk Ł, Kopaczek J, Rockett TBO, Richards RD, Kudrawiec R. Deep-level defects in n-type GaAsBi alloys grown by molecular beam epitaxy at low temperature and their influence on optical properties. Scientific Reports 2017; 7(1):12824. doi:10.1038/s41598-017-13191-9

35 Alberi K, Fluegel B, Beaton DA, Steger M, Crooker SA et al. Origin of deep localization in $GaAs_{1-x}Bi_x$ and its consequences for alloy properties. Physical Review Materials 2018; 2(11):114603. doi:10.1103/PhysRevMaterials.2.114603

36 Zhao CZ, Wei T, Sun XD, Wang SS, Wang J. The factors determining the band gap energy of the As-rich $GaBi_xAs_{1-x}$. Applied Physics A 2019; 125(2): 145. doi: 10.1007/s00339-019-2452-9

37 Yue L, Zhang X, Ou W, Shen Z, Wang S. Molecular beam epitaxy growth and properties of GaAsBi and AlAsBi. In: Wang S, Lu P (editor). Bismuth-Containing Alloys and Nanostructures. Singapore: Springer, 2019, pp. 11-36.

38 Christian TM, Alberi K, Beaton DA, Fluegel B, Mascarenhas A. Spectrally resolved localized states in $GaAs_{1-x}Bi_x$. Japanese Journal of Applied Physics 2017; 56 (3):035801. doi:10.7567/JJAP.56.035801

39 Saarinen K, Hautojärvi P, Lanki P, Corbel C. Ionization levels of As vacancies in as-grown GaAs studied by positron-lifetime spectroscopy. Physical Review B 1991; 44(19):10585. doi:10.1103/PhysRevB.44.10585

40 Hozhabri N, Sharma SC, Pathak RN, Alavi K. Defects in molecular beam epitaxial GaAs grown at low temperatures. Journal of Electronic Materials 1994; 23(6):519-523. doi:10.1007/BF02670654

41 Markov I. Kinetics of surfactant-mediated epitaxial growth. Physical Review B 1994; 50(15): 11271. doi:10.1103/PhysRevB.50.11271

42 Adamcyk M, Ballestad A, Young EC, Schmid JH, Tiedje T et al. Surfactant enhanced growth of GaNAs and InGaNAs using a Bi flux. In: International Conference on Molecular Bean Epitaxy; San Francisco, USA; 2002. pp. 275-276.

43 Gregory IS, Tey CM, Cullis AG, Evans MJ, Beere HE et al. Two-trap model for carrier lifetime and resistivity behavior in partially annealed GaAs grown at low temperature. Physical Review B 2006; 73(19):195201. doi:10.1103/PhysRevB.73.195201

44 Liliental-Weber Z, Lin XW, Washburn J, Schaff W. Rapid thermal annealing of low-temperature GaAs layers. Applied Physics Letters 1995; 66(16): 2086. doi:10.1063/1.113911